

TN-1403
AD-A017 699

Technical Note N-1403

KINK FORMATION AND ROTATIONAL RESPONSE OF SINGLE
AND MULTISTRAND ELECTROMECHANICAL CABLES

By

F. C. Liu

October 1975



Sponsored by

NAVAL FACILITIES ENGINEERING COMMAND

Approved for public release; distribution unlimited.

CIVIL ENGINEERING LABORATORY
Naval Construction Battalion Center
Port Hueneme, California 93043

Unclassified

SECURITY CLASSIFICATION OF THIS PAGE (When Data Entered)

REPORT DOCUMENTATION PAGE		READ INSTRUCTIONS BEFORE COMPLETING FORM
1. REPORT NUMBER TN-1403	2. GOVT ACCESSION NO. DN487004	3. RECIPIENT'S CATALOG NUMBER
4. TITLE (and Subtitle) KINK FORMATION AND ROTATIONAL RESPONSE OF SINGLE AND MULTISTRAND ELECTRO- MECHANICAL CABLES		5. TYPE OF REPORT & PERIOD COVERED Final; July 1973-June 1974
7. AUTHOR(s) F. C. Liu		6. PERFORMING ORG. REPORT NUMBER
9. PERFORMING ORGANIZATION NAME AND ADDRESS CIVIL ENGINEERING LABORATORY Naval Construction Battalion Center Port Hueneme, California 93043		8. CONTRACT OR GRANT NUMBER(s)
11. CONTROLLING OFFICE NAME AND ADDRESS Naval Facilities Engineering Command Alexandria, Virginia 22332		10. PROGRAM ELEMENT PROJECT, TASK AREA & WORK UNIT NUMBERS 62759N; YF52.556.004.01.001
14. MONITORING AGENCY NAME & ADDRESS (if different from Controlling Office)		12. REPORT DATE October 1975
		13. NUMBER OF PAGES 37
		15. SECURITY CLASS. (of this report) Unclassified
		15a. DECLASSIFICATION/DOWNGRADING SCHEDULE
16. DISTRIBUTION STATEMENT (of this Report) Approved for public release; distribution unlimited.		
17. DISTRIBUTION STATEMENT (of the abstract entered in Block 20, if different from Report)		
18. SUPPLEMENTARY NOTES		
19. KEY WORDS (Continue on reverse side if necessary and identify by block number) Electromechanical cables, wire ropes, stress analysis, cable kinks, cable rotations, cable mechanics, cable testing, cable modeling.		
20. ABSTRACT (Continue on reverse side if necessary and identify by block number) Mathematical models for double-armored and multistrand cables were formulated to simulate straight cable sections. Numerical solutions for free-end and fixed-end cables under tension were obtained with a computer. Controlled cable tests were conducted to generate data on the rotational behavior of six cables of different size and construction. Part of the data was used to compare with results from the analytical models. Experimental <div style="text-align: right;">continued</div>		

DD FORM 1 JAN 73 1473 EDITION OF 1 NOV 65 IS OBSOLETE

Unclassified

SECURITY CLASSIFICATION OF THIS PAGE (When Data Entered)



20. Continued

results and model predictions for elongation and rotation were in good agreement for the case of a double-armored cable. Experimental and predicted values of rotation for a 3×19 nonrotating, multistrand cable were not in good agreement, apparently because of the difficulty in modeling the complex construction of the cable. Two types of cables were subjected to constant tension and were twisted until kinks developed. These test results show that the buckling criterion for a solid rod can be used as a criterion for kinking of double-armored and multistrand cables.

Library Card

Civil Engineering Laboratory

KINK FORMATION AND ROTATIONAL RESPONSE
OF SINGLE AND MULTISTRAND ELECTROMECHANICAL
CABLES (Final), by F. C. Liu

TN-1403

37 p. illus

October 1975

Unclassified

1. Electromechanical cables

2. Single and multistrand

I. YF52.556.004.01.001

Mathematical models for double-armored and multistrand cables were formulated to simulate straight cable sections. Numerical solutions for free-end and fixed-end cables under tension were obtained with a computer. Controlled cable tests were conducted to generate data on the rotational behavior of six cables of different size and construction. Part of the data was used to compare with results from the analytical models. Experimental results and model predictions for elongation and rotation were in good agreement for the case of a double-armored cable. Experimental and predicted values of rotation for a 3×19 nonrotating, multistrand cable were not in good agreement, apparently because of the difficulty in modeling the complex construction of the cable. Two types of cables were subjected to constant tension and were twisted until kinks developed. These test results show that the buckling criterion for a solid rod can be used as a criterion for kinking of double-armored and multistrand cables.

CONTENTS

	Page
INTRODUCTION	1
CABLE MODELING	2
Single Helix	2
Double-armored Cable With Specified Tension and Rotation . .	4
Double-armored Cable With Specified Tension and Torque . . .	5
Multistrand Cable With Specified Tension and Rotation	5
Multistrand Cable With Specified Tension and Torque	7
Programs RADAC and RAMSC	8
CABLE TESTS	8
KINKING CHARACTERISTICS	9
Kinking Criterion Formulation	9
Kinking Tests	11
Examples of Kinking Prediction	13
FINDINGS AND CONCLUSIONS	13
RECOMMENDATIONS	14
REFERENCES	14
BIBLIOGRAPHY	15
NOMENCLATURE	18

LIST OF ILLUSTRATIONS

Figure 1. Developed triangle of a single helix wire.	20
Figure 2. External loadings and internal stresses on a single helix wire.	21
Figure 3. Developed double triangle for double-layered, contrahelically wound cables.	22
Figure 4. Tension versus elongation of 1x48 double-armored cable in fixed-end test.	23

List of Illustrations (Continued)

	Page
Figure 5. Torque versus elongation of 1x48 double-armored cable in fixed-end test, both positive and negative rotation.	24
Figure 6. Torque versus end rotation of 1x48 double-armored cable replotted from fixed-end test results.	25
Figure 7. Tension versus rotation of 1x48 double-armored cable in free-end test.	26
Figure 8. Tension versus elongation of 3x19 multistrand cable in fixed-end test.	27
Figure 9. Torque versus elongation of 3x19 multistrand cable in fixed-end test.	28
Figure 10. Torque versus rotation of 3x19 multistrand cable replotted from fixed-end test results.	29
Figure 11. Tension versus rotation of 3x19 multistrand cable in free-end test.	30
Figure 12. End termination for 3x19 cable, showing cable clamp used.	31
Figure 13. Hookup arrangement for torquing bar, weights, and test sample.	31
Figure 14. Kink formation on 3x19 cable.	31
Figure 15. Example of torque and tension data recorded during forced laying up of a 5/8-inch double-armored cable.	32
Figure 16. Stages of kink formation on 1x48 cable during negative torquing.	33
Figure 17. Various stages of kink formation on 1x48 double-armored cable during positive torquing.	33
Figure 18. Dimensionless kinking criterion for 3x19 and 1x48 electromechanical cables.	34

LIST OF TABLES

	Page
Table 1. Physical Properties of Cable Samples	35
Table 2. Cable End Conditions for the Measurement of Rotational Properties	36
Table 3. Value of EI for 1x48 and 3x19 Cables	36



INTRODUCTION

A kinked cable can jeopardize the performance of an undersea cable system, which may contain valuable data and hardware. Repair of such systems is costly and difficult (if not impossible in some cases). Therefore, the cable components in such systems must be properly designed to assure kink-free operation. Simulation of cable performance by use of mathematical models can prove a valuable designing tool. Rotational behavior and likelihood of kinking of a cable before its fabrication can be predicted.

After a cable is constructed, data on potential rotation and kink formation are needed to develop proper procedures for handling the cable during ship loading and deployment.

In addition, it may be feasible to replace cable testing by analytical predictions and thereby save cost and time.

A kink in a wire rope or a metallic electromechanical cable may be defined as a tight twist or curl resulting from rotation about the cable axis. Usually, a kink will cause electrical failure or mechanical damage or both. Preventing the formation of such undesirable deformations is essential for successful cable deployment.

Although the mechanism of kink formation in complex cables is not fully understood, an appreciation of the kinking problem can be obtained from a simple demonstration with a rubber band. Fix one end of a rubber band and twist the other end until a kink is formed. Then apply some tension and observe the kink being pulled out. Twist the rubber band more and a kink will form again. This simple demonstration shows that a kink will form at a critical twist or torque corresponding to a particular value of tension. A wire rope or cable is an elastic body, and it is reasonable to assume that there also exists a critical tension or a critical torque for kinking as with the rubber band. The main difference between a cable and a rubber band is the complex wire structure in the cable compared with the homogeneous rubber material.

Torque is needed to form a kink. Where does the torque come from? The history of loading on the cable determines the amount of residual torque. For example, when a payload is being lowered into the ocean, end rotation may occur due to the weight of the payload or the payload hydrodynamic movement. Torque at this time is zero until the payload reaches the seafloor where the tension suddenly is reduced to zero. Now, the rotation which occurred converts to end torque. Kinks form to release this end torque. Therefore, for kink-free operation, torque-balanced cable and slow lowering speeds are essential. However, this rule of thumb is not adequate for operations requiring high reliability. The criterion for cable kinking must be established and acceptable external loadings specified to assure safe operation.

This study includes both an analytical development and laboratory tests to determine the rotational behavior and kinking mechanism of several typical electromechanical (EM) cables. A kinking criterion applicable to most EM cables is established.

CABLE MODELING

A cable generally consists of one or more layers of helical strands wound around a core strand.* The mechanics of a single helix are first studied before formulating models for the more complex cable structure.

Single Helix

A single helix is defined by the arc length S , the length of the helical wire, and the pitch angle α , the angle that the wire makes with a horizontal line. The helix wire can be rolled out on a plane. With a vertical line drawn parallel to the strand axis from the top of the helix and a horizontal line at the lower end of the wire, a triangle is formed (Figure 1). The length of the helix is L . The pitch of the helix wire is P and the number of turns is $n = L/P$. A negative pitch length represents a left-lay helix. The length of the horizontal base is $X = 2\pi nR$, where R is the helix radius. As long as the wire remains helical, the developed triangle is a right triangle [1]. When the wire is tensioned, the helix radius tends to decrease due to the radial force generated by the wire tension. The combination of wire elongation and change in helix radius results in a change in n , which is a measure of end rotation of the helix. If the end is restrained, then a torque will be generated in the wire. Now consider what happens when a torque is applied at the ends of a helix wire. The torque causes an end rotation and wire elongation which, in turn, changes the internal stresses and geometry. The combination of tensile and torsional loadings causes a complex change in cable configuration.

The main assumptions in the following derivation are that the wire geometry remains helical and symmetrical after deformation and that friction forces are neglected. Other assumptions are as follows:

1. Wire material follows Hooke's law.
2. Wire lateral deformation due to contact stress is negligible.
3. Wire radius reduction due to Poisson's effect is negligible.
4. Strengths of conductors, dielectrics, fillers, jackets, and other nonstrength members are negligible.

Consider now a simple helix under axial tension F and torque T ; Prime indicates the state after loading. The pitch angle α changes to α' , and the wire length S changes to S' . The helix has been stretched and twisted, and the curvature of the helix changes from $\kappa = \cos^2 \alpha / R$ to $\kappa' = \cos^2 \alpha' / R'$. The torsion or twist of the helix changes from $\tau = \cos \alpha \sin \alpha / R$ to $\tau' = \cos \alpha' \sin \alpha' / R'$. These deformations signify changes in wire tension and torque. The wire tension p due to change in wire length S is

* A strand generally consists of one or more layers of helical wires wound around a core wire.

$$p = \frac{S' - S}{S} AE \quad (1)$$

where E = Young's modulus of elasticity
A = Cross sectional area

Phillips and Costello developed [2] the twisting and bending moments due to changes in torsion and curvature as:

$$M_t = \frac{\pi E r^4}{4(1 + \nu)} (\tau' - \tau) \quad (2)$$

and

$$M_b = \frac{\pi E r^4}{4} (\kappa' - \kappa) \quad (3)$$

where r = radius of wire
 ν = Poisson's ratio

A force in the binormal direction is generated by this geometrical change.

$$B = M_t \kappa' - M_b \tau' \quad (4)$$

Thus, knowing the change in S and α , one can calculate the wire tension p, torque M_t , bending moment M_b , and binormal force B. With given external boundary conditions, these internal stresses are computed and used in the equilibrium equations to solve for the external deflections of the whole strand. All external and internal forces and moments are shown in Figure 2. A minimum helical radius R_m is reached when adjacent wires of the same helix radius touch each other. This condition has been derived by Phillips and Costello [2].

$$R_m = r [1 + \cot^2 \frac{\pi}{m} \csc^2 \alpha]^{1/2} \quad (5)$$

where m = number of wires in a strand.

This radius is used as the minimum radius of a wire helix in the numerical calculations. For a strand with solid core, if the core helical radius is larger than the calculated minimum radius, then the core radius is used in the calculations. For double-armored cables, the outer wire must conform with the inner wire in helical radius. In complex multistrand cables, such as 3x19, the minimum radius of various wire layers becomes difficult to determine due to their complex geometrical arrangements. Fortunately, the strand has a solid core so that the minimum radius of each wire can be computed without using Equation 5.

Double-armored Cable With Specified Tension and Rotation

There are four variables of major interest: the external tension F , end torque T , elongation ΔL , and rotation ϕ . Two of these variables can be fixed by prescribing boundary conditions, or external loadings. The remaining two are the unknown reactions. In this case the unknown reactions are end torque and elongation. These external cable reactions can be determined once the geometry of the loaded helical wires is determined. Each developed triangle for a loaded helix may be defined by α_1' and S_1' . For double-armored cable the four unknowns are α_1' , α_2' , S_1' and S_2' . Four equations are needed to define the cable configuration.

Since both layers of wire must elongate the same axial length, based on the developed triangle concept in Figure 3, there is a constraint:

$$L_1' = L_2'$$

or

$$S_1' \sin \alpha_1' = S_2' \sin \alpha_2' \quad (6)$$

where subscripts 1 and 2 indicate inner and outer layer, respectively.

Another constraint may be derived from the condition that there will be no relative rotation between layers, that is $\phi_1 = \phi_2 = \phi$. From Figure 3 the rotation equations are:

$$S_1' \cos \alpha_1' = R_1' (2\pi n_1 + \phi) \quad (7)$$

$$S_2' \cos \alpha_2' = R_2' (2\pi n_2 + \phi) \quad (8)$$

The pitch radius R_1' is governed by Equation 5 and the pitch radius of the adjacent wire layer.

The axial force equilibrium equation requires the balance of external and internal forces.

$$\begin{aligned} F = m_1 (p_1 \sin \alpha_1' + B_1 \cos \alpha_1') \\ + m_2 (p_2 \sin \alpha_2' + B_2 \cos \alpha_2') \end{aligned} \quad (9)$$

The wire tension p_1 is related to S_1' by Equation 1. The binormal forces B_1 and B_2 are computed from Equation 4.

Equations 6, 7, 8, and 9 were solved numerically for α_1' , α_2' , S_1' and S_2' by iteration. First assume S_1' and α_1' , using Equation 6, 7, and 8 for the iteration of α_1' . After α_1' is determined, α_2' and S_2' are calculated. Then Equation 9 is used to check the assumed S_1' .

The end torque T is calculated based on the external torque-balance equation:

$$T = m_1 (M_{a1} - M_{c1} + M_{t1} \sin \alpha_1' + M_{b1} \cos \alpha_1') \\ + m_2 (M_{a2} - M_{c2} + M_{t2} \sin \alpha_2' + M_{b2} \cos \alpha_2') \quad (10)$$

where $M_a = p R' \cos \alpha'$

$$M_c = B R' \sin \alpha'$$

The torsional and bending moments, M_{ti} and M_{bi} , caused by the change in wire helix are computed from Equations 2 and 3. Elongation is calculated from

$$\Delta L = L_1' - L_1 = L_2' - L_2 \quad (11)$$

Double-armored Cable With Specified Tension and Torque

The two external variables to be determined are elongation and end rotation, both of which can be expressed again in terms of α_1' , α_2' , S_1' and S_2' . The four equations for solving the four unknowns are:

1. Uniform elongation: Equation 6
2. Uniform rotation: From Equations 7 and 8, eliminating ϕ ,

$$\frac{S_1' \cos \alpha_1'}{R_1'} - 2\pi n_1 = \frac{S_2' \cos \alpha_2'}{R_2'} - 2\pi n_2$$

3. Axial force equilibrium: Equation 9
4. Axial torque equilibrium: Equation 10

After solving for α_1' , α_2' , S_1' , and S_2' , by iteration the rotation is calculated by Equation 7 or 8 and the elongation is calculated by Equation 11.

Multistrand Cable With Specified Tension and Rotation

Based on the same principle used in solving the double-armored cable, the helix geometry after loading is determined first.

The variables needed to determine the unknown end conditions of a multistrand cable are the wire pitch lengths S_i and pitch angles α_i as well as the strand pitch length S_s and pitch angle β . For a 3x19

cable there are six variables to be determined: α_1' , α_2' , β' , S_1' and S_2' and S_s' . In order to simplify the equations, the double helical wires were treated as single helical wires. Uniform elongation of all wires in a strand gave the following condition.

$$S_1' \sin \alpha_1' = S_s' \quad (12a)$$

$$S_2' \sin \alpha_2' = S_s' \quad (12b)$$

The consistency of rotation requires that the end rotation of all wires, (ϕ_i) must be equal to the strand rotation ϕ_s . For a specified end rotation ϕ , the condition is:

$$\phi_1 = \phi_2 = \phi_s = \phi$$

where

$$\phi_1 = \frac{S_1'}{R_1'} \cos \alpha_1' - 2\pi n_1 \quad (13a)$$

$$\phi_2 = \frac{S_2'}{R_2'} \cos \alpha_2' - 2\pi n_2 \quad (13b)$$

$$\phi_s = \frac{S_s'}{R_s'} \cos \beta' + 2\pi n_s \quad (13c)$$

Subscripts 1, 2, and s indicate inner layer, outer layer, and core or strand, respectively.

The last equation needed to solve for the six unknowns is the axial force equilibrium equation:

$$F = m_s \left[m_1 C_1 + m_2 C_2 + p_c \right] \sin \beta' + B_s \sin \left(\frac{\pi}{2} + \beta' \right) \quad (14)$$

$$\text{where } C_1 = p_1 \sin \alpha_1' + B_1 \sin \left(\frac{\pi}{2} + \alpha_1' \right)$$

$$C_2 = p_2 \sin \alpha_2' + B_2 \sin \left(\frac{\pi}{2} + \alpha_2' \right)$$

The binormal forces in the wires, B_1 , B_2 and B_s , caused by the change in wire curvature and torsion are computed from Equation 4. The wire stresses p_1 and p_s are related to wire lengths S_1' and S_s' by Equation 1.

From equations 12a, 12b, 13a, 13b, 13c, and 14, the values of α_1 , α_2' , and β' and S_1' , S_2' and S_s' may be obtained by iteration.

The end torque is calculated from the following equation for torque equilibrium:

$$T = m_s [m_1 C_3 + m_2 C_4 + C_5] \quad (15)$$

$$\text{where } C_3 = p_1 R_s' \sin \alpha_1' \cos \beta' + p_1 R_1' \cos \alpha_1' \sin \beta'$$

$$+ M_{b1} \sin \left(\frac{\pi}{2} + \alpha_1' \right) \sin \beta' + M_{t1} \sin \beta' \sin \alpha_1'$$

$$+ B_1 R_s' \sin \left(\frac{\pi}{2} + \alpha_1' \right) \cos \beta' + B_1 R_1' \cos \left(\frac{\pi}{2} + \alpha_1' \right) \sin \beta'$$

$$C_4 = p_2 R_s' \sin \alpha_2' \cos \beta' + p_2 R_2' \cos \alpha_2' \sin \beta'$$

$$+ M_{b2} \sin \left(\frac{\pi}{2} + \alpha_2' \right) \sin \beta' + M_{t2} \sin \beta' \sin \alpha_2'$$

$$+ B_2 R_s' \sin \left(\frac{\pi}{2} + \alpha_2' \right) \cos \beta' + B_2 R_2' \cos \left(\frac{\pi}{2} + \alpha_2' \right) \sin \beta'$$

$$C_5 = p_s R_s' \cos \beta' + M_{ts} \sin \beta' + M_{bc} \sin \left(\frac{\pi}{2} + \beta' \right)$$

$$+ B_s R_s' \cos \left(\frac{\pi}{2} + \beta' \right)$$

Wire torsional and bending moments M_{t1} and M_{b1} which are induced by the change in helix geometry are computed from Equations 2 and 3. The elongation is computed from

$$\Delta L = S_s' \sin \beta' - S_s \sin \beta \quad (16)$$

Multistrand Cable With Specified Tension and Torque

Again, the end reactions are to be determined from the six unknown variables: α_1' , α_2' , β , S_1' , S_2' and S_s' . The six equations are:

1. Uniform elongation criterion: Equation 12 (two equations)
2. Constant rotation condition: Equation 15 (two equations
- eliminating ϕ)
3. Force equilibrium: Equation 14
4. Torque equilibrium: Equation 15

These six equations are solved by iteration.

Finally, the end rotation is calculated using Equation 13 and the elongation by Equation 16.

Programs RADAC and RAMSC

Based on the mathematic developments, computer programs RADAC and RAMSC were written to analyze the double-armored and multistrand cables, respectively. The computer programs simulate the laboratory cable tests used to obtain rotational and torsional data. They can be used to determine the rotational and extensional response to a combined tensile and torsional loading. The rotational stiffness can be estimated using these programs without actual cable testing.

Detailed cable construction dimensions and wire material elastic properties are needed as input. The programs compute the elongation and end rotation or torque for a predetermined tension increment. These programs are available on loan from CEL.

CABLE TESTS

The main purpose of the cable testing program was to generate reliable data on the rotational response of electromechanical cables commonly in use. These data have three applications: first, to predict kinking; second, to verify analytical cable models; and finally, to design, select, specify, and improve the handling of future electromechanical cables.

Six cables were selected for rotational property measurements, and their essential mechanical properties are presented in Table 1. They cover the spectrum of typical oceanic electromechanical cables in use today. Availability was an important factor that affected cable selection (for example, the newly developed Kevlar cables were not available for measurement). By selecting these cables and measuring their rotational properties, representative sampling of the majority of electromechanical cables was obtained.

The tests were conducted at the Naval Research Laboratory using the method and facilities described in detail in Reference 3; the test samples were 6 feet long. An extension tower was added to the top end of the standard 60,000-pound test machine. The elongation was measured by the Electro-optical Extensometer, and the top of the lower end socket was used as a lower target. The rotation was monitored by a dial attached to a lockable swivel at the lower end. The tension and torque were measured by a load cell at the top end. The end sockets of the test samples were potted with zinc. Two X-Y plotters were used to plot the tension-versus-elongation and torque-versus-elongation curves.

Each cable went through the conventional axial stress-strain test with end conditions as specified in Table 2.

The free-end tests were characterized by a zero moment in the cable. Based on this principle, free-end tests can be conducted in a regular test machine. The method involved a trial-and-error procedure. The lower end rotation was adjusted until the torque reading was zero. The process was repeated for different tension loadings to develop a free-end

stress/rotation curve. In this test, the elongation was not measured because the cable rotation caused rotation of the target of the photo electrical measuring instrument.

The results of the cable tests are reported in Reference 4. The extensional and rotational response data for the 5/8-inch 1x48 double-armored cable and the jacketed, 1/2-inch, 3x19, torque-balanced cable are also presented in this report in Figures 4 through 11. Also shown in these figures are data predicted by RADAC and RAMSC. The free-end rotation data are an indication of the degree of torque-balancing. Negative rotation is in the direction to unlay the outer wire or strand. The fixed-end test data include the tension-versus-rotation and the torque-versus-rotation curves. The slope of the torque-versus-rotation curve is defined as the rotational stiffness, an important parameter affecting the kinking of a cable. Note that the rotational stiffness for the 1x48 double-armored cable has different values for different directions of rotation (Figure 6). The cable becomes very soft when the outer layer is unlaying. The rotational stiffness of the 3x19 multistrand cable is nearly constant like a solid rod (Figure 10).

Program RADAC predicts both the elongation and the rotation of a double-armored cable to reasonable accuracy, but program RAMSC which simulates a multistrand cable can only predict the elongation to the desired accuracy of $\pm 5\%$. A significant difference was found between the predicted and measured values of end rotation. Specifically, although the magnitudes of the the measured and predicted rotations were in reasonable agreement, the directions of rotation were opposite. The difference was about 14 degree/ft. The predicted rotation indicated a slight overbalance; i.e., the predicted resistance to unlaying was greater than actually occurred. This difference may result from the assumption that the stress distribution of a helical strand is the same as in a straight strand. In reality, wires closer to the center of the cable have higher stresses; therefore, the resultant tension over the strand is closer to the center of the cable, and the positive torque developed by the tension is less. If the average torque developed within each strand is assumed not to change, the total positive cable torque is less than predicted. The predicted rotation will always represent a slight overbalance compared to that of the measured value. The reason manufacturers design 3x19 cables with a built-in overbalance may be to account for such a loss. Other factors that may affect the analytic result include the presence of inter-wire or inter-strand friction, the change in helical radius under load, the jacket stiffness, and the accuracies of input wire dimensions, pitch angles, and elastic properties.

Program RADAC and program RAMSC have been combined into program TAWAC.

KINKING CHARACTERISTICS

Kinking Criterion Formulation

Both Vachon [6] and Hearle [7] recommend the use of Timoshenko's buckling criterion for a slender rod [8] to predict the onset of cable

or yarn kinking. The buckling criterion for a circular rod according to Timoshenko is:

$$\left(\frac{\frac{T_c}{2\pi EI}}{L} \right)^2 + \frac{\frac{C}{\pi^2 EI}}{\frac{L^2}{L^2}} = 1 \quad (17)$$

where T_c = end torque

L = length of rod

E = Young's modulus of elasticity

I = Moment of inertia about diameter, $I = I_p / 2$

I_p = Moment of inertia about rod center

C = axial compression force.

Since, for cable kinking, tension F_c (instead of compression C) is applied, the equation becomes

$$\left(\frac{\frac{T_c}{2\pi EI}}{L} \right)^2 = 1 + \frac{\frac{F_c}{\pi^2 EI}}{\frac{L^2}{L^2}}$$

where $F_c = -C$

Now, the axial force restrains the buckling action. In actual use, the cable is long enough and the tension large enough that

$$\frac{F_c L^2}{\pi^2 EI} \gg 1$$

(see Figure 11), and the buckling criterion becomes

$$\left(\frac{\frac{T_c}{2\pi EI}}{L} \right)^2 = \frac{\frac{F_c}{\pi^2 EI}}{\frac{L^2}{L^2}} \quad (18)$$

The term $2\pi EI/L$ is the Greenhill torque T_g , the torque at which a rod will buckle under torque alone. The term $(\pi/L)^2 EI$ is the Euler compression force F_e , the axial force needed to buckle a rod. For cable kinking, the Greenhill torque still provides a buckling criterion, but the Euler compression has little real meaning as the axial force is now in tension. Since the terms $(2\pi/L)EI$ and $(\pi/L)^2 EI$ embody the torsional and

bending stiffnesses, they are used to nondimensionalize the external torque T and axial force F . From Equation 18, the critical tension is expressed as:

$$F_c = \frac{T_c^2}{4 EI} \quad (18a)$$

Kinking Tests

Kinking experiments were conducted on samples cut from two electromechanical cables of different construction. The 1x48 double-armored cable and the 3x19 multistrand cable were selected as test samples. In the experiments combined tension and torsional loadings were applied to the cable, and the measurement taken of the rotational response and the cable tension and torque when a kink formed. The sample length varied from 21 feet to 23 feet 9 inches. Swaged eyes were used as end terminations for the double-armored cables, and cable clamps were used for the multi-strand cables (Figure 12 and 13). The cable samples were suspended under a steel frame 30 feet from the ground; a torquing bar and a known weight were attached to the lower end. The torque was measured by two low-range spring scales attached to the torquing bar. The weight was first attached to the torquing bar, and the cable was allowed to rotate to an equilibrium orientation. Starting from that orientation, two men, each positioned at one end of the torquing bar, walked in a circle to apply torsion and rotation to the lower end of the cable. The cable sample was eventually twisted into a kink and the experiment stopped (Figure 14). The torque and rotation were recorded at desired intervals. Finally the rotation and torque at the kink were recorded. The sample was changed and a new experiment started.

In some of the experiments, the tension and the torque were continuously monitored by a load cell connected to a strip chart recorder. The torque variation during the formation of the kinds was observed and recorded (Figure 15). Photographs were taken during the experiments to facilitate the study of the configuration of various kinds of cable deformation at various load combinations. In addition, the mechanism of kink formation and its variations were observed and recorded.

The process of cable kinking is more complex than the simple buckling of a short rod. For a rod, both the axial compression force and the torque tend to accelerate the failure of the rods. Once an initial eccentricity is created by the torque, the compression force alone could complete the buckling process by producing higher and higher bending moment through increasing eccentricity. This is not so for cable kinking where the axial force is not compressive. Instead, a tension acts on the cable to reduce any initial eccentricity caused by the torque. Therefore, larger torque is needed to curl the cable into a helical-shape. As the torque increases, the cable deforms locally at a weak point and a half loop is formed. The torsion-induced bending moment is balanced by the tension-induced resisting

moment. As the torque continues to increase, the resisting moment also increases and finally reaches a maximum. This is the point for the onset of kinking. Further increase in torque will result in a rapid formation of a complete loop with one or more turns (Figure 16). Thus, the exterior torque is relieved somewhat. The configuration of the loop formed depends mainly on the tension and torque on the cable. When a homogeneous elastic rod is subjected to low tension and high torsion, the ends of the rod rotate opposite to one another and the axis of the rod gradually becomes helical. After a certain number of turns, a loop with a small radius and a helical twist will form at a weak point in the rod. Such a loop may be called a kink. A rope or cable behaves in a similar way when it is under low tension and high torsion. Such deformations have been observed in 3x19 cables in both rotational directions and in 1x48 cables during negative rotation. When the 1x48 double-armored cable is subjected to low tension and high torsion in positive rotation, the outer layer contracts whereas the inner layer expands resulting in high contact stresses between the layers. Further, torsional loading increases these stresses and eventually the wires in the inner layer buckle and push through a weak opening in the outer layer (Figure 17). Such buckling of the inner wires causes considerable reduction in torsion. Further increases in torsion produce additional failures, usually distributed at equal intervals, until finally a kink is formed at one of the failure points. Thus, the positively rotating 1x48 cable does not behave like the 3x19 cable or the negatively rotating 1x48 cable.

The results of the twist experiment are presented in nondimensional form. The tension is divided by the Euler compression force, which has no physical meaning here. The torque is divided by the Greenhill torque, which is the torque required to buckle a cylinder by twisting alone. With the assumption that the cable behaves like a solid rod, the value of EI may be derived from the torque-versus-rotation curves obtained during the twist tests, assuming that $I = I_p/2$ where I_p is the polar moment of inertia of the cable cross section. The criteria for kinking of the 1x48 and 3x19 cables are summarized in Figure 18. Most data points follow the theoretical buckling criterion (Equation 18a) except those for the positive twist of the 1x48 cable. This is expected since the kinking mechanism for the 1x48 cable in the positive direction is different from the rest of the cable-twisting tests as discussed previously. Therefore, for cables that do not fail prematurely due to the construction of the cable or other factors, the following empirical formula describes the average kinking criterion:

$$F_c = \frac{3T_c^2}{8EI} \quad (19)$$

Note that if $I = I_p/3$ instead of $I = I_p/2$ for a cable cross section, the empirical formula would match Timoshenko's buckling criterion exactly.

$$F_c = \frac{T_c^2}{4EI} \quad (18a)$$

Example of Kinking Prediction

A 1/2-inch, 3x19, torque-free cable is selected to deploy an instrument package to the seafloor 10,000 feet below the surface. The package weighs 5,000 pounds in seawater. Evaluate the possibility of kinking when the lift line becomes slack.

From Figure 11, the free-end rotation rate with a 5,000-pound dead weight is -40 degrees per 72 inches of cable length, or -6.67 degrees per foot. The total rotation during the free-end deployment to 10,000 feet is the -185 revolutions. From Figure 10, the corresponding torque is about -5 in.-lb at near slack conditions. It will now be determined whether this amount of torque is sufficient to form a kink and, if required, the tension needed to prevent kinking. The value of the cable-bending stiffness is found to be 1,200 lb-in.² and according to Equation 18a, the critical tension for a -5 in.-lb torque is 0.0078 pound. This small torque is not sufficient to cause any wire bending or twisting failures. The lower end of the cable may form large radius loops on the seafloor but it will not form kinks that cannot be pulled out by increasing the tension. No wire failures are expected.

FINDINGS AND CONCLUSIONS:

1. The extensional and rotational response of contrahelically wound, double-armored electromechanical cable to external loadings and deformations can be satisfactorily simulated by an analytical model such as the one presented in this report.
2. The extensional response of multistrand cables can be satisfactorily predicted by the analytical model presented in this report but the rotational response for a nearly non-rotational multistrand cable can not be predicted accurately without precise knowledge of the cable's internal dimensions. Because the amount of rotation for such cables will be small, precise prediction of such rotation may not be required.
3. A relationship between critical tension and critical torque, as derived from the cylinder buckling criterion and verified by laboratory test data, can be expressed by the following formula:

$$F_c = T_c^2 / 4EI$$

This formula shows that the critical tension can be minimized by maximizing the bending stiffness and minimizing the external torque. The magnitude of external torque can be minimized by minimizing the tension-induced rotation.

4. Rotational testing of six different types and sizes of cable showed that cables of similar construction can exhibit quite different rotational characteristics. A double-armored construction is not necessarily torque-balanced and a multistrand construction can be non-rotational. Data on tension versus elongation and torque versus rotation are not sufficient for an adequate description of the cable rotational properties.

RECOMMENDATIONS

1. Equation 18a should be used whenever possible to determine the critical tension needed to prevent the formation of kinks. The critical torque, which is the tension-induced torque, in most cases, can be obtained from laboratory test data or from Program TAWAC.
2. Equation 18a shows that increasing the bending stiffness will reduce the likelihood of kink formation. Therefore, within the flexibility requirements of sheave bending, deployment cables should be selected which have the largest possible bending stiffness.
3. When rotational data are not available and Equation 18a can not be used, a deck winch capable of providing a minimum line tension of 100 pounds at the lower end should be used to prevent cable kinking.
4. The analytical cable models developed in this report are recommended as a tool for optimal cable design and selection.

REFERENCES

1. M. Chi. "Analysis of operating characteristics of strands in tension allowing end-rotation," paper presented at Winter Annual Meeting of American Society of Mechanical Engineers, New York, New York, Nov 1972. (ASME paper no. 72-WA/Oct-19)
2. J. W. Phillips and G. A. Costello. "Contact stresses in twisted wire cables," ASCE Proceedings, Journal of the Engineering Mechanics Division, vol 99, no. EM2, Apr 1973, pp 331-341.
3. Naval Research Laboratory. Memorandum Report 2459: Method of measuring the mechanical behavior of wire rope, by D. A. Milburn and N. J. Randler. Washington, DC, Jul 1972.
4. ———. Memorandum Report 2903: Tensile and torsional characteristics of electromechanical cables, by Roy K. Samrus. Washington, DC, Nov 1974.
5. Massachusetts Institute of Technology, Charles Stark Draper Laboratory. Report E-2497: Kink formation properties and other mechanical characteristics of oceanographic strands and wire rope, by W. A. Vachon. Cambridge, Massachusetts, Apr 1970.
6. ———. Group 38 Report: Kink formation in long cables as an extension of the buckling theory of slender bars, by W. A. Vachon. Cambridge, Massachusetts, 1968 (unpublished report).
7. J. W. S. Hearle. "Structural mechanics of torque-stretch yarns: The mechanism of snarl formation," Journal of Textile Institute Transactions, vol 57, no. 10, Oct 1966, pp T441-T460.
8. Timoshenko, S. Theory of Elastic stability. New York, New York, McGraw Hill Inc., 1936, p 169.

BIBLIOGRAPHY

- Bert, C. W., and R. A. Stein (1962). "Stress analysis of wire rope in tension and torsion," Wire and Wire Products, vol 37 (May 1962, pp 621-624; Jun 1962, pp 769-770, 772, 816).
- Charlson, A. D., R. G. Kasper, and M. A. Tucchio (1973). A structural analysis of a multi-conductor cable, Naval Underwater Systems Center, Technical Report 4549. Newport, Rhode Island, Sep 1973.
- Chi, M. (1971). Analysis of operating characteristics of strands in tension allowing end rotation, Catholic University of America, Report 71-10. Washington, DC, Sep 1971.
- Chi, M. (1971). An analysis of multi-wire strands in tension and combined torsion, Catholic University of America, Report 71-9. Washington, DC, Sep 1971.
- Durelli, A. J., and S. Machida (1972). Response of oversized epoxy strand models to axial, torsional, and bending loads, Catholic University of America, Report 72-2. Washington, DC, Feb 1972.
- Engel, Von E. (1958). "Das Drehbestreben der Seile und ihre Drehsteifigkeit, Oesterreichische Ingenieur-Zeitschrift, vol 1, no. 1, Jan 1958, pp 33-39.
- Gibson, P. T., H. A. Cress, W. J. Kaufman, and W. E. Gallent (1969). "Torsional properties of wire rope," paper presented at American Society of Mechanical Engineers, New York, New York, May 1969. (ASME paper no. 69-DE-34)
- Hall, H. M. (1951). "Stresses in small wire ropes," Wire, Mar 1951, pp 228, 257-259.
- Hearle, J. W. S. (1958). "The mechanics of twisted yarns: The influence of transverse forces on tensile behavior," Journal of Textile Institute Transactions, vol 49, 1958, pp T389-T408.
- Hearle, J. W. S. (1966). "Structural mechanics of torque-stretch yarns: The mechanism of snarl formation," Journal of Textile Institute Transactions, vol 57, no. 10, Oct 1966, pp T441-T460.
- Hearle, J. W. S. (1969). "On the theory of the mechanics of twisted yarns," Journal of Textile Institute Transactions, vol 60, no. 3, Mar 1969, pp 95-101.
- Hearle, J. W. S., H. M. A. E. El-Behery, and V. M. Thakur (1961). "The mechanics of twisted yarns: Theoretical developments," Journal of Textile Institute Transactions, vol 52, no. 5, May 1961, pp T197-T220.
- Hearle, J. W. S., P. Grasber, and B. Backer (1969). Structural mechanics of fibers, yarns, and fabrics, vol 1. New York, New York, Wiley-Interscience, 1969.
- Hearle, J. W. S. and A. E. Yegin (1972). "The snarling of highly twisted monofilaments. Part I: The load-elongation behavior with normal snarling," Journal of Textile Institute Transactions, vol 63, no. 9, Sep 1972.

- Heller, S. R., Jr., M. Chi, and C. Ome (1972). Torsion of a fluted bar with a rope-like cross-section, Catholic University of America, Report 72-10. Washington, DC, 1972.
- Hruska, F. H. (1951). "Calculation of stresses in wire rope," Wire and Wire Products, vol 26, Sep 1951, pp 766-767, 799-801.
- Hruska, F. H. (1952). "Radial forces in wire rope," Wire and Wire Products, vol 27, May 1952, pp 459-463.
- Hruska, F. H. (1953). "Tangential forces in wire rope," Wire and Wire Products, vol 28, May 1953, pp 455-460.
- Kasper, R. G. (1973). Cable design guidelines based on a bending, tension and torsion study of an electromechanical cable, Naval Underwater Systems Center, Technical Report 4619, New London, Connecticut, Oct 1973.
- Layland, C. L., A. R. S. Rao, and H. A. Ramsdale (1953). "Experimental investigation of torsion in stranded mining wire ropes," in Proceedings of Institution of Mechanical Engineers, vol 1, no. 8, 1952-1953, pp 323-336.
- Leissa, A. W. (1959). "Contact stresses in wire ropes," Wire and Wire Products, vol 34, Mar 1959, pp 307-314, 372-373.
- Machida, S., and A. J. Durelli (1972). Response of a strand to axial and torsional displacements, Catholic University of America, Report 72-1. Washington, DC, Jan 1972.
- Milburn, D. A., and N. J. Rendler (1972). Method of measuring the mechanical behavior of wire rope, Naval Research Laboratory, Memo Report 2495. Washington, DC, Jul 1972.
- Minor, John C., Philip T. Gibson, and H. A. Cress (1972). Experimental investigations of electromechanical cable, Battelle Memorial Institute. Long Beach, CA, Feb 1972.
- Nowak, Gerhard (1974). "Computer design of electromechanical cables for ocean applications," in Proceedings of Tenth Annual Marine Technology Society Conference, Washington, DC, 1974, pp 293-305.
- Paul, W. (1970). Review of synthetic fiber ropes, United States Coast Guard Academy. New London, Connecticut, Aug 1970.
- Phillips, J. W., and G. A. Costello (1973). "Contact stresses in twisted wire cables," ASCE Proceedings, Journal of Engineering, Mechanics Division, vol 99, no. EM2, Apr 1973, pp 331-341.
- Platt, M. M. (1950). "Mechanics of elastic performance of textile materials, Part VI: Influence of yarn twist on modulus of elasticity," Textile Research Journal, vol 20, no. 10, Oct 1950, pp 660-667.
- Platt, M. M., W. G. Klein, and W. J. Hamburger (1958). "Mechanics of elastic performance of textile materials, Part XIII: Torque development in yarn systems: single yarn," Textile Research Journal, vol 28, no. 1, Jan 1958, pp 1-14.

Riding, G., and N. Wilson (1965). "The stress-strain properties of continuous filament yarns," Journal of Textile Institute, vol 56, 1965, p T205.

Seely, F. B., and J. O. Smith (1952). Advanced mechanics of materials, 2nd ed. New York, New York, John Wiley and Sons, 1952.

Stein, R. A., and C. W. Bert (1962). "Radius of curvature of a double helix," Journal of Engineering for Industry, Aug 1962.

Treloar, L. R. G., and G. Riding (1963). "A. Theory of the stress-strain properties of continuous filament yarns," Journal of Textile Institute, vol. 54, 1963, p T156.

Vachon, W. (1968). Loop formation in long cables as an extension of the buckling theory of slender bars, Massachusetts Institute of Technology, Instrumentation Laboratory, Group 38 Report. Cambridge, Massachusetts, 1968.

Vachon, W. (1970). Kink formation properties and other mechanical characteristics of oceanographic strands and wire rope, Massachusetts Institute of Technology, Charles Stark Draper Laboratory, Report E-2497. Cambridge, Massachusetts, Apr 1970.

Added in proof:

Knapp, R. H. Nonlinear analysis of a multi-wire cable with nonuniform mechanical properties in tension and torsion, Paper presented in Marine Technology Society Annual Meeting, San Diego, Sep 1975.

NOMENCLATURE

A	Cross-sectional area of load-bearing wire
B	Binormal force in wire (lb)
C	Axial compression force (lb)
E	Young's modulus of elasticity of wire material (psi)
F	External axial force (lb)
F_c	Critical tension for kinking (lb)
F_e	Euler compression $(\pi/L)^2 EI$ (lb)
I	Moment of inertia about cable diameter (in. ⁴)
I_p	Polar moment of inertia (in. ⁴)
L	Length of the strand or cable (in.)
ΔL	Cable elongation (in.)
M_b	Wire bending moment from curvature change (in.-lb)
M_n	Wire bending moment component in the normal direction (in.-lb)
M_t	Wire axial torque from end torsion (in.-lb)
m	Number of wires in a layer or number of strands in a layer
N	Normal tension component (lb)
n	Pitch number
R	Helix radius (in.)
R_m	Minimum helix radius of a wire (in.)
r	Radius of wire cross section (in.)
P	Pitch length of wire or strand (in.)
p	Axial tension in wire (lb)
S	Arc length of load-bearing wire (in.)
T	External axial torque (in.-lb)
T_c	Critical torque for kinking (lb)

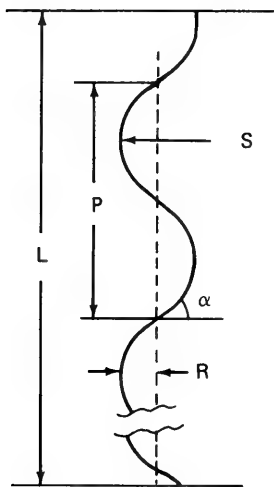
T_g	Greenhill torque, $\frac{2\pi EI}{L}$ (in.-lb)
X	Base of developed triangle (in.)
α	Wire angle from horizontal, rad
β	Strand angle from horizontal rad
κ	Curvature of wire (in. ⁻¹)
ν	Poisson's ratio
τ	Torsion of wire (radians/in.)
ϕ	End rotation, radian

Subscripts

1	First layer from core, inner layer
2	Second layer from core, outer layer
i	i th layer from core
s	Strand

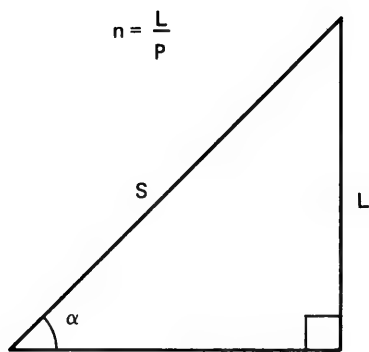
Superscript

'	Prime indicates loaded state
---	------------------------------



Helix geometry

(a)



Developed triangle

(b)

Figure 1. Developed triangle of a single helix wire.

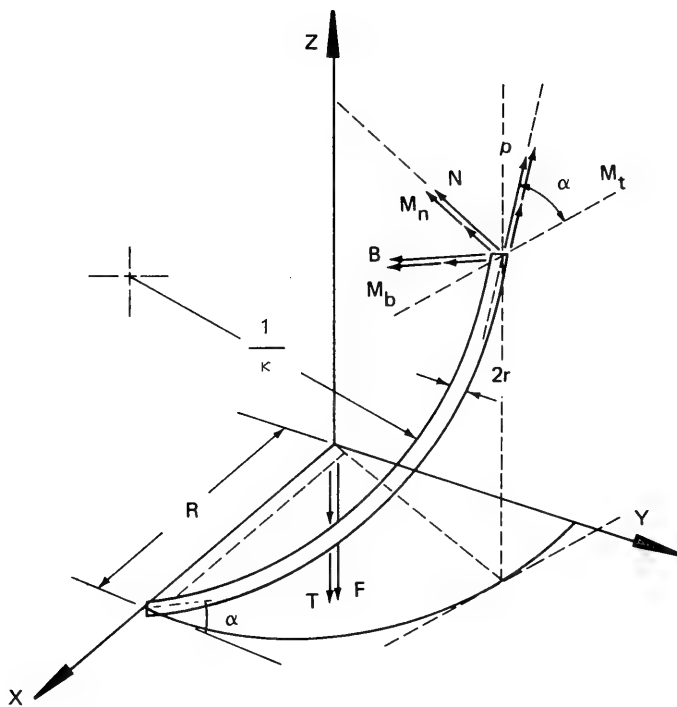


Figure 2. External loadings and internal stresses on a single helix wire.

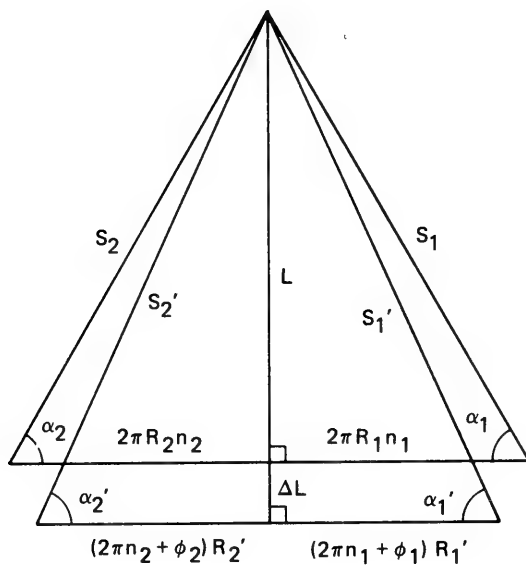
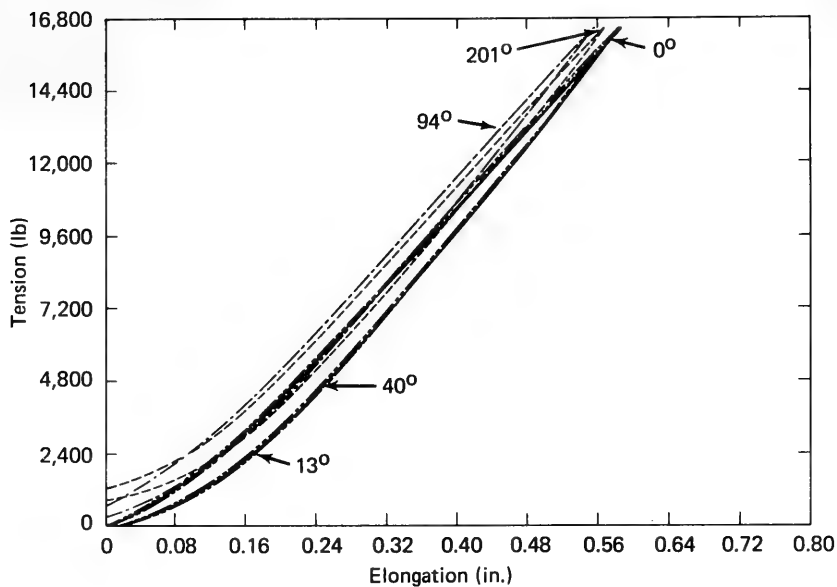
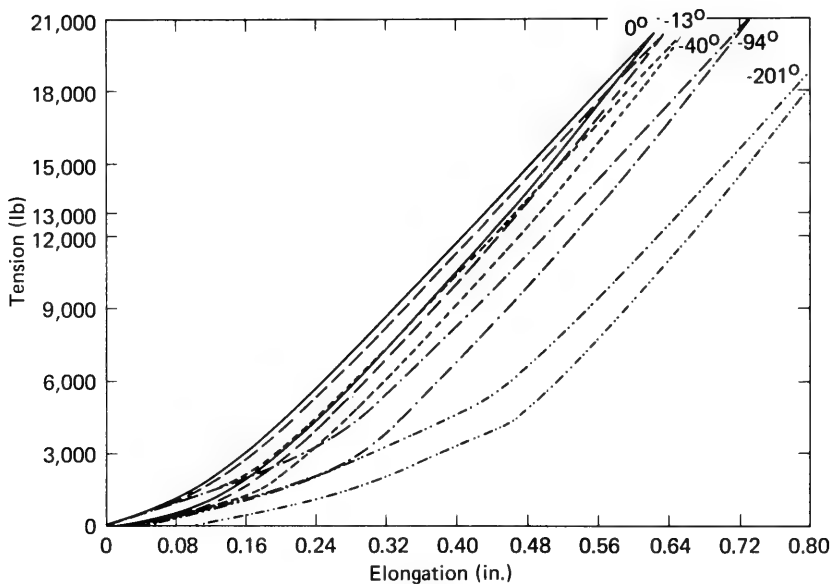


Figure 3. Developed double triangle for double-layered, contrahelically wound cables.



(a) Positive rotation



(b) Negative rotation

Figure 4. Tension versus elongation of 1x48 double-armored cable in fixed-end test.

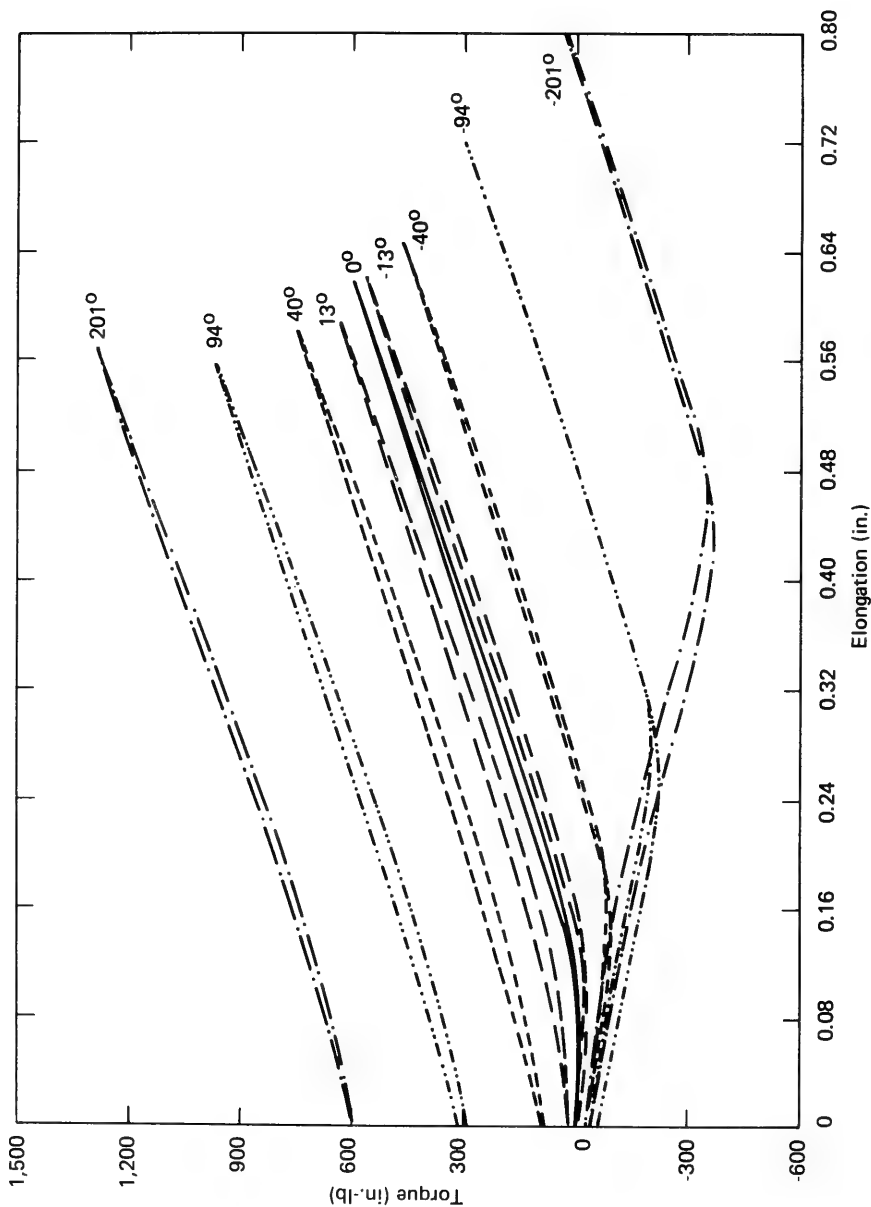


Figure 5. Torque versus elongation of 1x48 double-armored cable in fixed-end test, both positive and negative rotation.

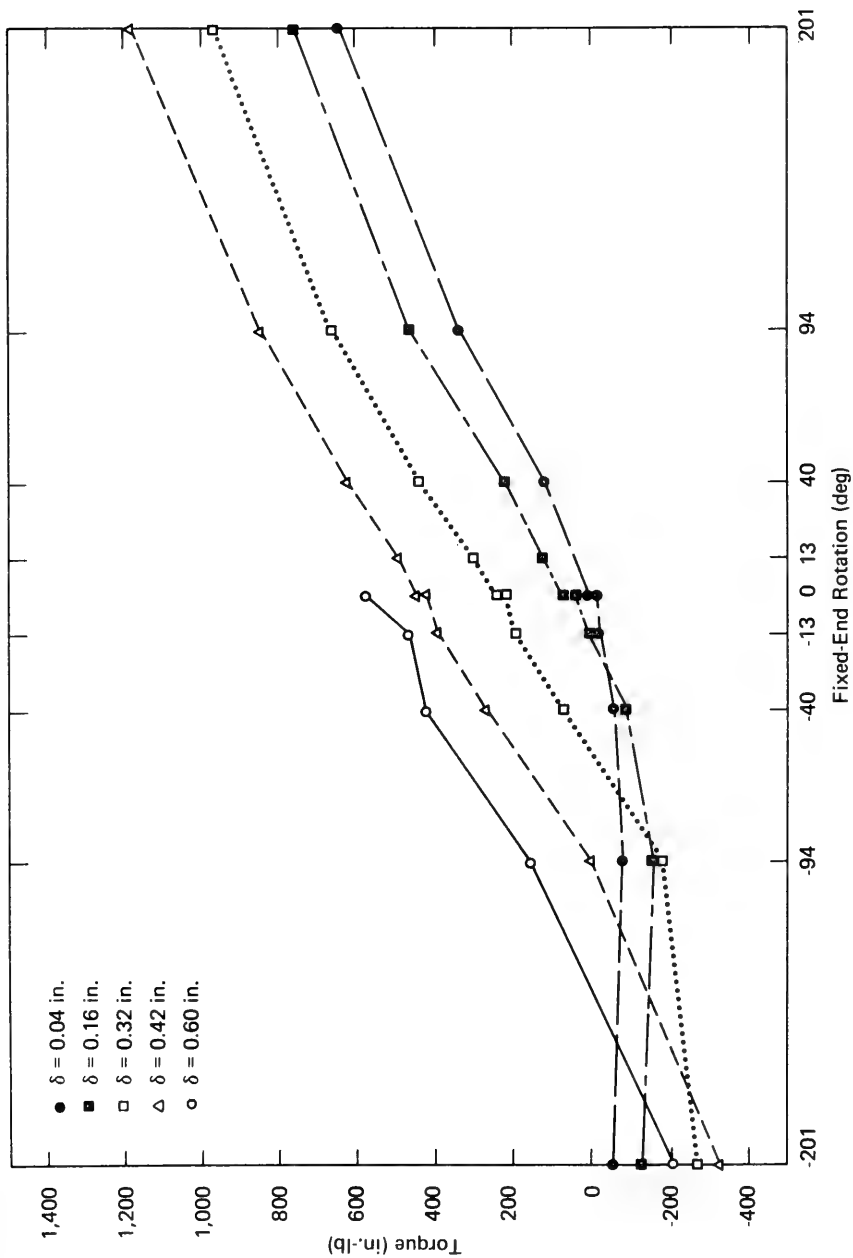


Figure 6. Torque versus end rotation of 1x48 double-armored cable replotted from fixed-end test results.

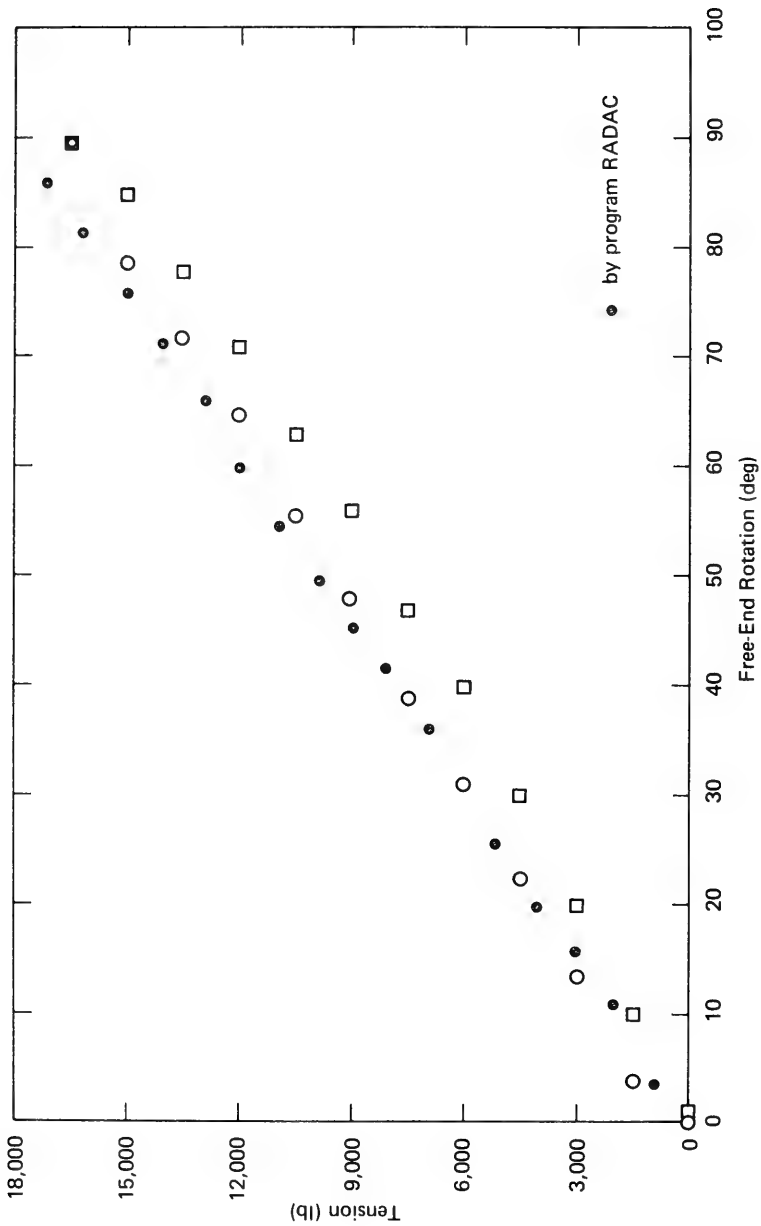
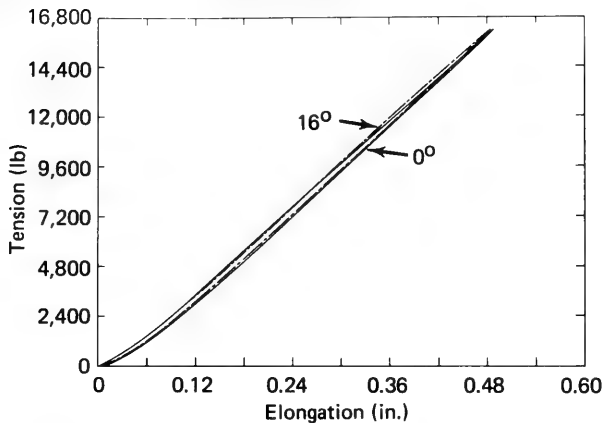
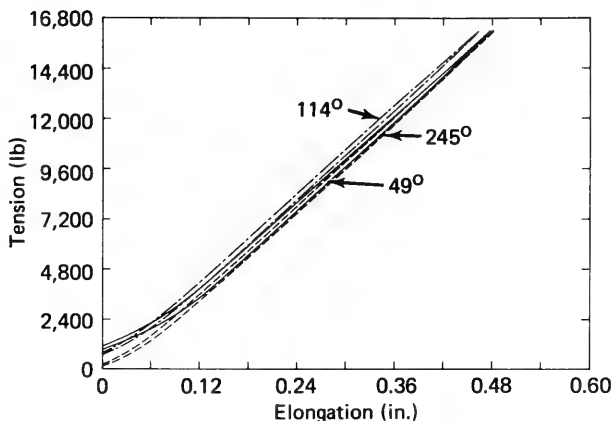


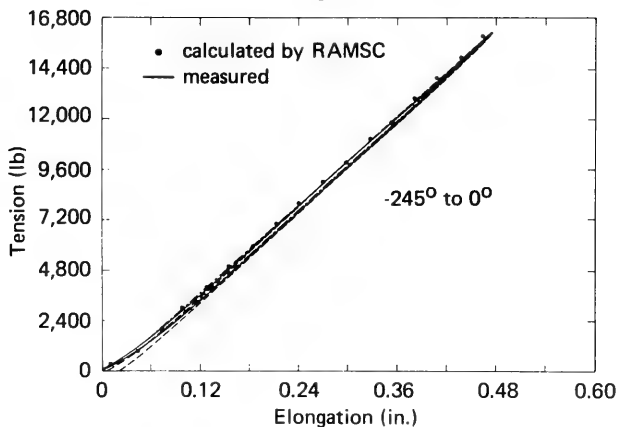
Figure 7. Tension versus rotation of 1x48 double-armored cable in free-end test.



(a) Positive rotation,
0 and 16 degrees



(b) Positive rotation,
49, 114 and 245 degrees



(c) Negative rotation
for all degrees

Figure 8. Tension versus elongation of 3x19 multistrand cable in fixed-end test.

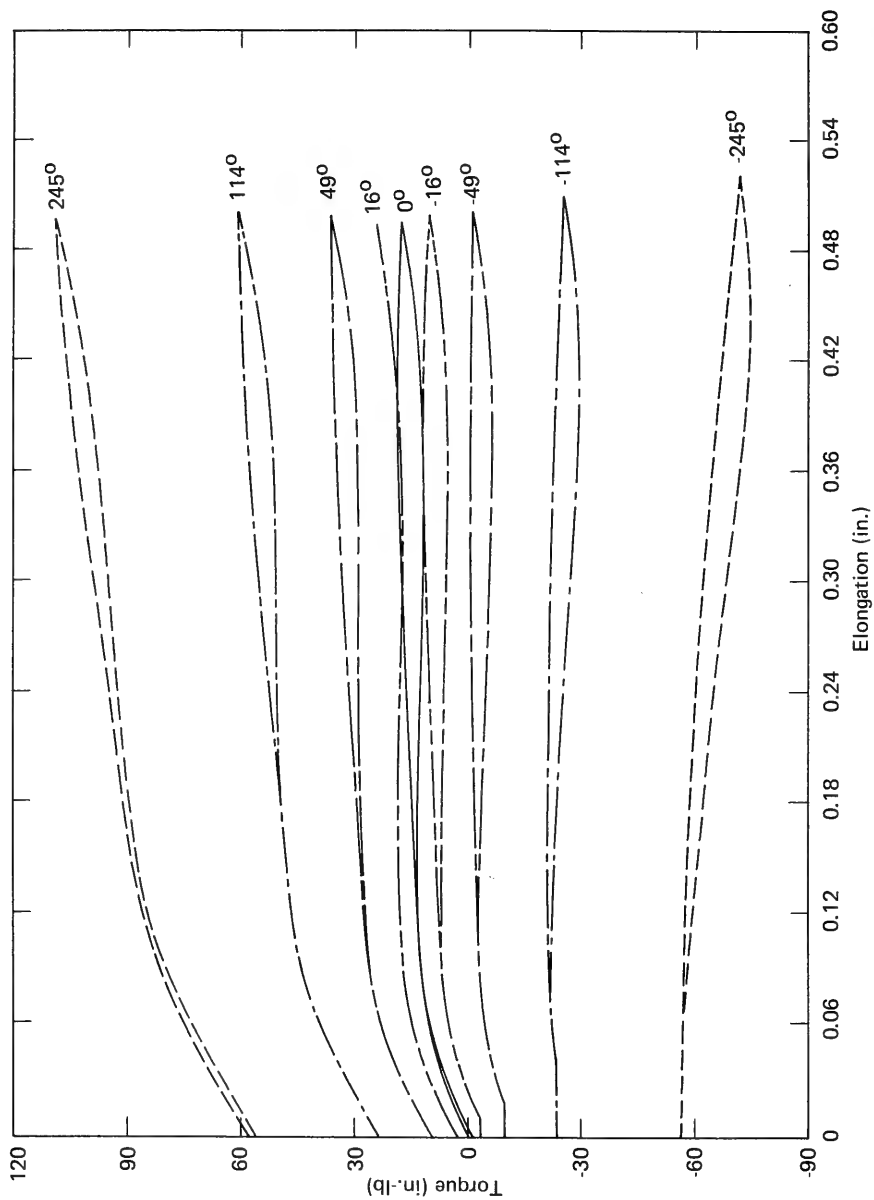


Figure 9. Torque versus elongation of 3x19 multistrand cable in fixed-end test.

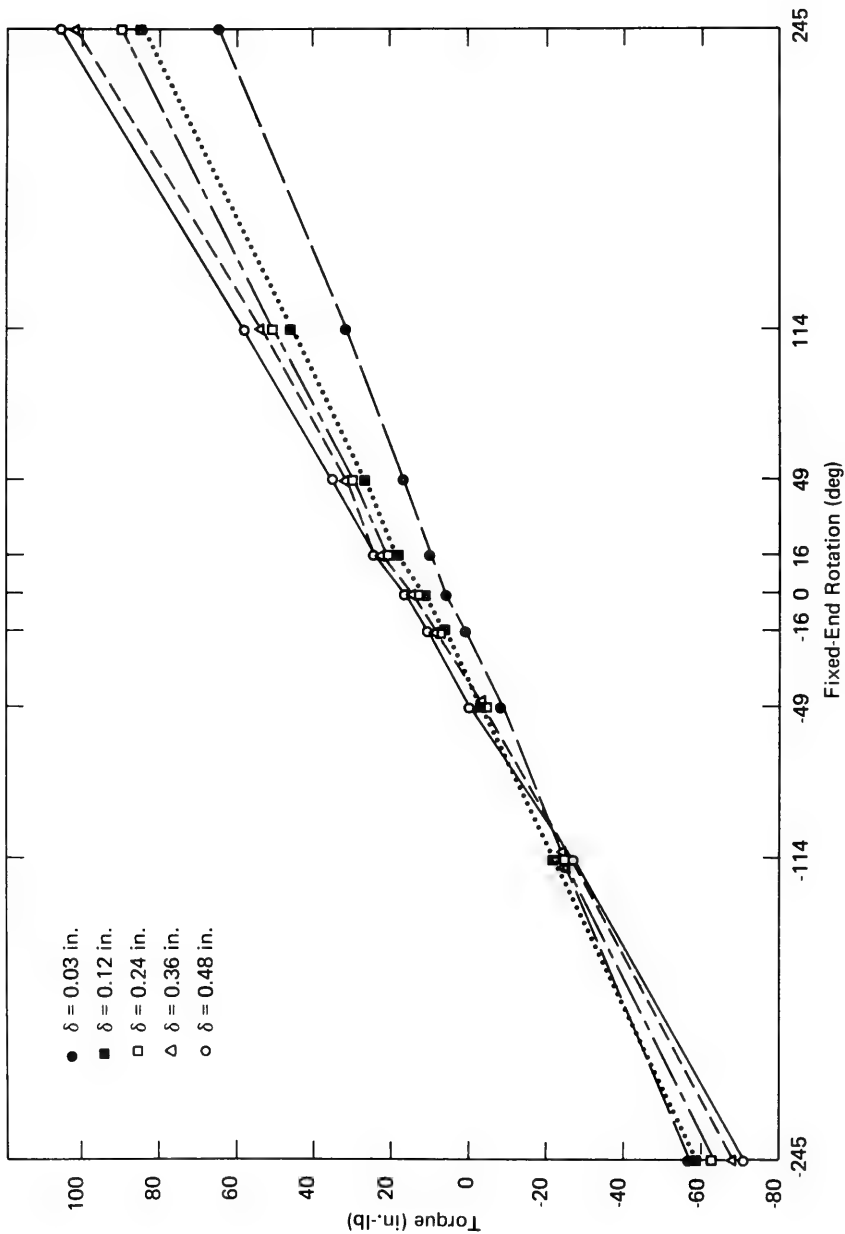


Figure 10. Torque versus rotation of 3x19 multistrand cable replotted from fixed-end test results.

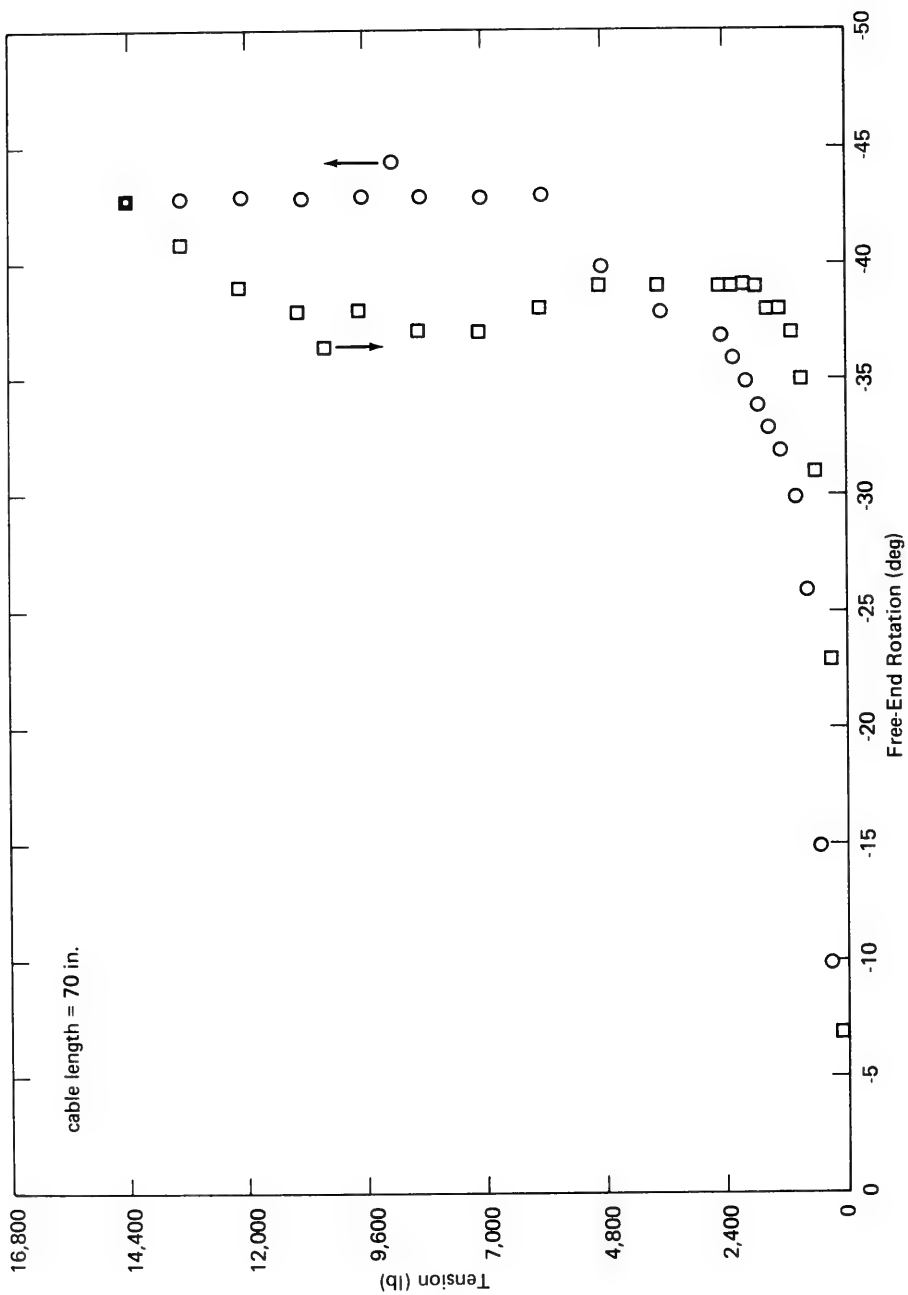


Figure 11. Tension versus rotation of 3x19 multistrand cable in free-end test.



Figure 12. End termination for 3x19 cable, showing cable clamp used.

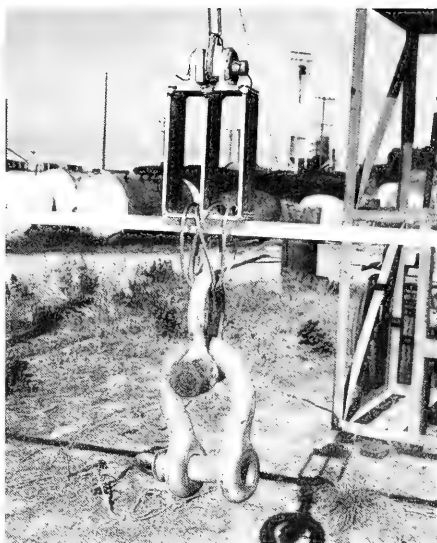


Figure 13. Hookup arrangement for torquing bar, weights, and test sample.



(a) Positive torque



(b) Negative torque

Figure 14. Kink formation on 3x19 cable.

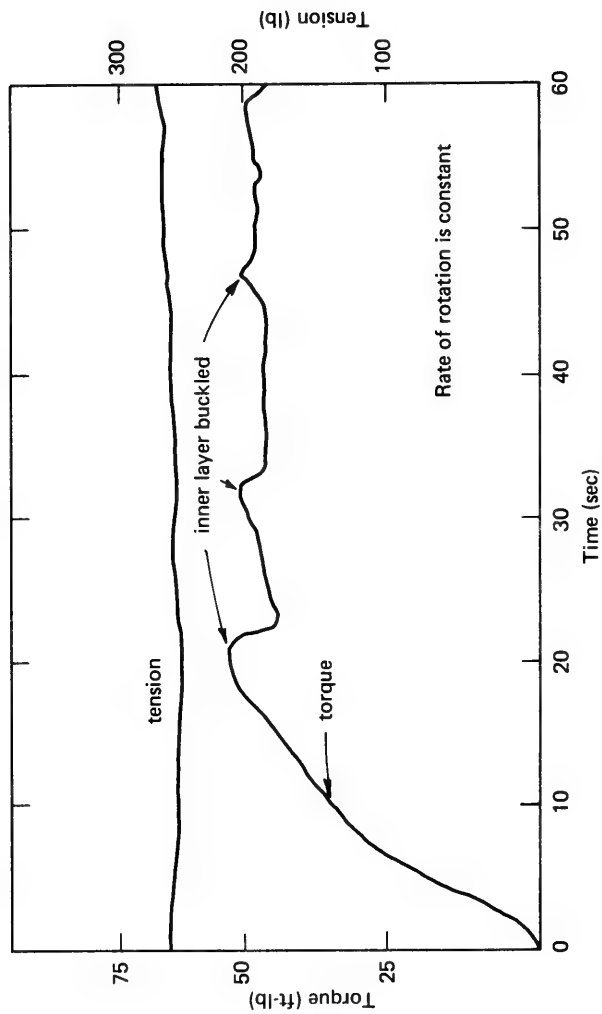


Figure 15. Example of torque and tension data recorded during forced laying up of a 5/8-inch double-armored cable.

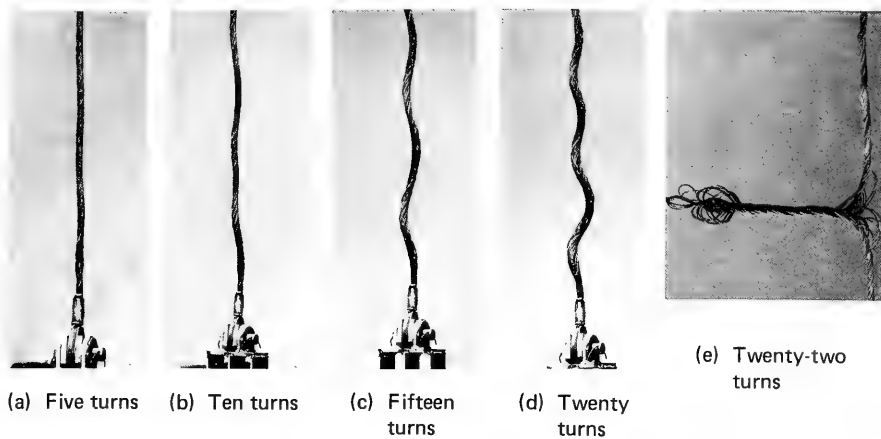


Figure 16. Stages of kink formation on 1x48 cable during negative torquing.

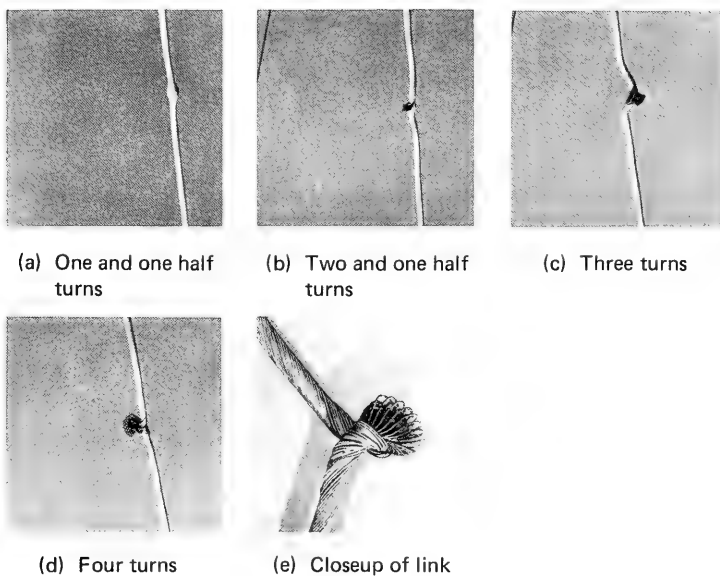


Figure 17. Various stages of kink formation on 1x48 double-armored cable during positive torquing.

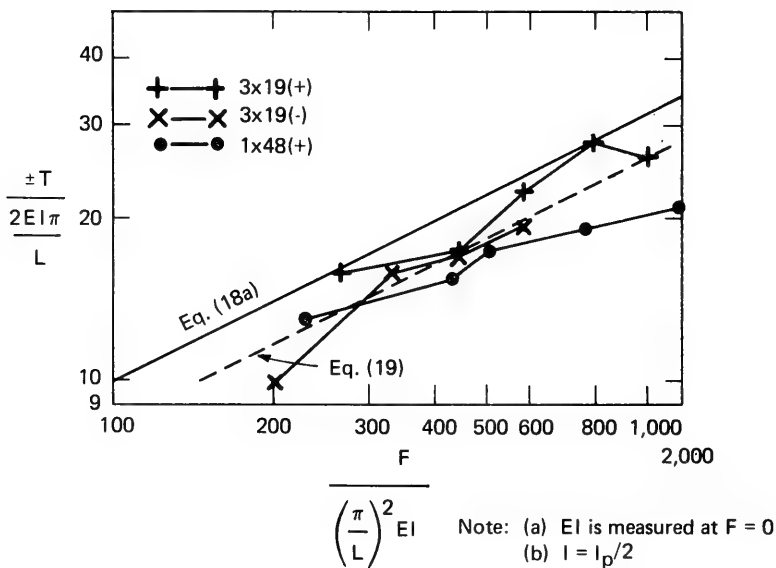


Figure 18. Dimensionless kinking criterion for 3x19 and 1x48 electromechanical cables.

Table 1. Physical Properties of Cable Samples

No.	Cable Samples	Specific Use or Location	Helix Parameters	Cable Construction Dimensions						Breaking Strength (psi)
				Strand	Wire Layer No. 0 (Core)	Wire Layer No. 1	Wire Layer No. 2	Wire Layer No. 3	Wire Layer No. 4	
1	1x48 galvanized IPS ^a torque balance	Sea Spider	Diameter (in.) Number Pitch radius Pitch length	5/8 1 0 ∞	none	0.056 24 0.237 4.16	0.071 24 0.301 5.687	— — — —	— — — —	32,000
2	3x19 nontorque with jacket	SEACON II	Diameter (in.) Number Pitch radius Pitch length	0.24 3 0.142 5.04	0.070 1 0 ∞	0.035 9 0.053 1.46	0.058 9 0.093 1.46	— — — —	— — — —	25,700
3	1x81	DOTIPOS	Diameter (in.) Number Pitch radius Pitch length	1.15 1 0 ∞	none	0.088 33 0.47 —	0.065 48 0.555 —	— — — —	— — — —	45,000
4	1x48 jacketed wire	Seafloor Deep Corer	Diameter (in.) Number Pitch radius Pitch length	1.5 1 0 ∞	none	0.117 24 0.48 —	0.102 24 0.665 —	— — — —	— — — —	130,000
5	1x41 high strength	Armorless Ocean Cable	Diameter (in.) Number Pitch radius Pitch length	0.3 1 0 ∞	0.069 1 0 ∞	0.041 8 0.056 6.0	0.039 8 0.089 6.0	0.030 8 0.095 6.0	0.047 16 0.128 6.0	16,000
6	6x19 IWRC ^b	Hoisting Rope	Diameter (in.) Number Pitch radius Pitch length	0.165 6 0.18 4.8	0.037 1 0 ∞	0.034 6 0.050 1.69	0.014 6 0.050 1.69	0.031 12 0.070 1.69	— — — —	26,600

^aImproved plowed steel.^bInner wire rope core.

Table 2. Cable End Conditions for the Measurement of Rotational Properties

Type of Cable	Diameter (in.)	Preset Angular Rotation for Fixed-End Tests (deg) –									Free-End Rotation Tests
		Run 1	Run 2	Run 3	Run 4	Run 5	Run 6	Run 7	Run 8	Run 9	
1x4	0.5	161	75	32	11	0	-11	-32	-75	-161	One end rotated manually to obtain zero torque
6x11	0.5	305	142	61	20	0	-20	-61	-142	-305	
3x19	0.5	265	114	49	16	0	-16	-49	-114	-265	
1x4	0.66	201	94	40	13	0	-13	-40	-94	-201	
1x81	1.5	79	39	19	9	0	-9	-19	-39	-79	
1x48	1.5	95	44	19	6	0	-6	-19	-44	-95	

Table 3. Value of EI for 1x48 and 3x19 Cables

Tension (lb)	EI (in. ² -lb)			
	Measured Rotation		Averaged Rotation	
	Positive	Negative	Positive	Negative
1x48 Double-Armored Cable				
1,022	38,600	1,760	38,600	1,940
522	38,500	1,980	37,000	1,850
256	30,600	1,480	31,900	1,580
139	20,400	1,210	27,500	1,350
91.5	24,600	1,700	25,200	1,220
59.5	22,700	1,060	22,500	1,105
49.5	22,706	1,060	21,800	1,070
27.5	18,850	1,215	19,400	970
3x19 Multistrand Torque-Balanced Cable				
30.5	906	1,530	980	1,530
51.5	965	1,790	990	1,760
69.5	1,250	1,850	1,020	1,960
91.5	1,020	2,270	1,060	2,180
112.5	1,100	—	1,080	—

DISTRIBUTION LIST

SNDL Code	No. of Activities	Total Copies	
-	1	12	Defense Documentation Center
FKAIC	1	10	Naval Facilities Engineering Command
FKNI	6	6	NAVFAC Engineering Field Divisions
FKN5	9	9	Public Works Centers
FA25	1	1	Public Works Center
-	6	6	RDT&E Liaison Officers at NAVFAC Engineering Field Divisions
-	222	224	CEL Special Distribution List No. 11 for persons and activities interested in reports on Ocean Engineering

